Computational and Structural Biotechnology Journal 18 (2020) 1210–1220

COMPUTATIONAL AND STRUCTURAL BIOTECHNOLOGY JOURNAL

journal homepage: www.elsevier.com/locate/csbj

The Contorsbody, an antibody format for agonism: Design, structure, and function

Guy J. Georges [a,*], Stefan Dengl [a], Alexander Bujotzek [a], Friederike Hesse [a], Jens A.A. Fischer [a], Achim Gärtner [a], Jörg Benz [b], Matthias E. Lauer [b], Philippe Ringler [c], Henning Stahlberg [c], Friederike Plath [d], Ulrich Brinkmann [a], Sabine Imhof-Jung [a]

[a] Roche Pharmaceutical Research and Early Development, Large Molecule Research, Roche Innovation Center Munich, Nonnenwald 2, 82377 Penzberg, Germany
[b] Roche Pharmaceutical Research and Early Development, Chemical Biology, Roche Innovation Center, Basel, Switzerland
[c] C-CINA, Center for Celullar Imaging and Nano Analytics, University of Basel, Switzerland
[d] Roche Pharmaceutical Research and Early Development, Pharma Technical Development, Roche Innovation Center, Basel, Switzerland

ARTICLE INFO

Article history:
Received 28 February 2020
Received in revised form 28 April 2020
Accepted 6 May 2020
Available online 14 May 2020

Keywords:
Antibody format
Molecular modeling
Receptor dimerization
Protein engineering
Electron microscopy
Molecular dynamic

ABSTRACT

The careful design of the antibody architecture is becoming more and more important, especially when the purpose is agonism. We present the design of a novel antibody format that is able to promote receptor dimerization and induce signal transduction resulting in cell proliferation. Mono-specific bivalent Y-shape IgGs made of two light chains and two heavy chains are engineered into single chain dimers of two modified heavy chains, resulting in the fixation of the two Fab fragments along the Fc dimerizing moiety. By this, an antagonist of the Her-receptor family, Trastuzumab, is re-formatted into an agonist by simply incorporating the original binding motif into a different geometrically and sterically constrained conformation. This novel format, named Contorsbody, retains antigen binding properties of the parental IgGs and can be produced by standard technologies established for recombinant IgGs. Structural analyses using molecular dynamics and electron microscopy are described to guide the initial design and to confirm the Contorsbody as a very compact molecule, respectively. Contorsbodies show increased rigidity compared to IgGs and their Fab moieties are positioned parallel and adjacent to each other. This geometry has an increased potential to trigger cell surface antigen or receptor 'cis'-dimerization without 'trans'-bridging of cells or mere receptor blockade.

1. Introduction

Therapeutic monoclonal antibodies (Mabs) are widely used to treat human diseases [18,30,15,16] because of their ability to bind the majority of disease-relevant targets and their suitability for engineering, especially as bispecifics [4]. Some Mabs can exhibit agonistic properties such as enhanced signaling triggered by membrane anchored receptors as exemplified by CD40 targeting antibodies [41]. Bivalency as a pre-requisite for agonistic activity was dissected a while ago [26]. An interesting review summarizing the numerous antibody engineering approaches from the last decades appeared recently [9]. However, more specific combination and/or engineering is often required in order to achieve a particular biological function, especially for agonistic purposes [24]. A couple of recent examples demonstrate that the format type and orientation are key to achieve receptor activation [38,46].

In this study, we describe the design, structural modeling and generation of a novel antibody format, termed Contorsbody. This format reduces the distance between the two binding motifs of an antibody and fixes them in a particular orientation while maintaining the basic properties of an immunoglobulin G (IgG). The term Contorsbody, a contraction of 'Contortion of the body', has been selected to contrast with the extended Y-shape of the antibody. The overall architecture of the Contorsbody is analyzed by electron microscopy (EM) in order to reveal more detailed structural parameters. The EM studies use a second Contorsbody for which the binder motifs are analog to Emactuzumab [32]; we called this one Contorsbody analog 2.

A Contorsbody with the V- and C-domains of Trastuzumab [7] serves as a prototype in this study to demonstrate a functionality switch. The standard IgG Trastuzumab binds the Her2 receptor that is overexpressed in breast cancer, in a way that it prevents

* Corresponding author.
E-mail address: guy.georges@roche.com (G.J. Georges).

https://doi.org/10.1016/j.csbj.2020.05.007

the homo-dimerization of the receptors. Hence, the molecule has antagonistic properties, blocks the signal transduction and thereby prevents cell proliferation [27,40,42]. However, Scheer et al. later demonstrated that when reformatted into a chemically linked bis-Fab, the resulting Trastuzumab-derived molecule is capable of inducing cell proliferation [36]. We got inspired by this example and transitioned the Trastuzumab IgG into the Contorsbody structure in order to validate the design.

We functionally characterized the Contorsbody in comparison to the parent Trastuzumab IgG. This study demonstrates that the format of an antibody can have a profound effect, i.e. inverting its original functionality.

2. Results and discussion

2.1. Design of sterically constrained IgG-like Contorsbodies

A regular IgG is composed of two heavy chains and two light chains (Fig. 1B); dimerized heavy chains form the antibody Fc part with disulfide bridges within the Fc hinge. The Contorsbody (Fig. 1A) harbors identical domains to IgGs, in the same stoichiometry, yet in a sterically confined format. Instead of being composed of two heavy(H) and two light(L) chains as an antibody (Fig. 1B), these molecules are homodimers of two H-L chain fusion proteins that dimerize through the Fc (CH2-CH3) regions. H- and L-chains are fused via linker peptides L1 and L2 composed of repeated G4S modules (Fig. 1C). Those linkers are inserted C-terminally of the CH1 domain and N-terminally to the second variable domain (VL) of the original light chain, thus flanking both structural ends of the Fc moiety. The prototype Contorsbody described here harbors IgG1 constant domains (CH1-CH2-CH3) and the V-regions of Trastuzumab. A structural model of the composition is depicted in Fig. 1D.

The Trastuzumab Contorsbody 3D model was built by connecting fragments from the protein databank (PDB). Two Trastuzumab Fabs (PDB ID 1N8Z [10]) are positioned alongside one Fc moiety (PDB ID 1HZH [35]) in a head to tail fashion; each Fab is connected by two extended double G4S linkers to one Fc half.

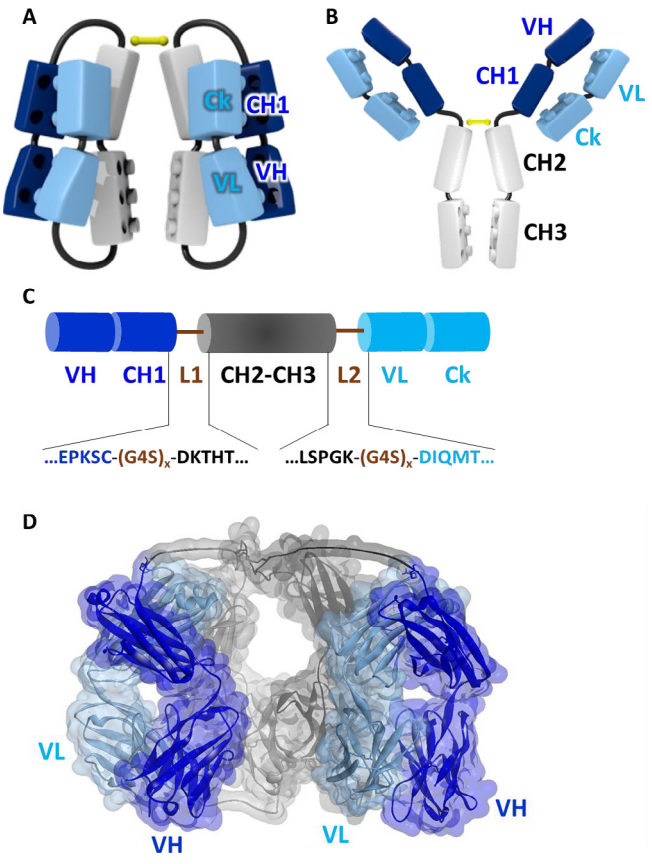

Fig. 1. A: Lego representation of the Contorsbody format. B: Lego representation of the heavy chain (dark blue and grey) and light chain (light blue). C: Representation of the linear sequence of the single chain Contorsbody with detailed composition of the linkers and the flanking amino acids. D: Contorsbody format molecular model. (For interpretation of the references to colour in this figure legend, the reader is referred to the web version of this article.)

2.2. Molecular dynamics helps to define the linker lengths

Modulating the lengths of the flexible L1 and L2 linkers is an obvious way of adjusting the structural parameters of the Contorsbody. Using molecular dynamics (MD) simulations, we evaluated the structural impact of several different linker lengths. Starting models are created with linkers L1 and L2 composed of G4S modules of one, two, or three repeats, respectively. The paratope to paratope distances are monitored over a simulation time of 100–200 ns at a temperature of 298 K. The results are shown in Fig. 2.

The Contorsbody with linker length 5 (one G4S unit) is highly constrained in its paratope to paratope distance so that the distance at simulation start is almost the same as the average over second half of the simulation. The variants with longer linkers show higher distance variability and seem to reach a metastable state only after approximately 80–90 ns simulation time. While paratope to paratope distances of up to 7.88 nm (linker length 10) and 10.05 nm (linker length 15) are being observed, the data clearly suggests that, in solvent, a compact conformation with paratope to paratope distances below 6 nm is the preferred one. The values are summarized in Table 1.

The short simulation spans observed here do not represent an exhaustive sampling of the conformational space of the Contorsbody; notably, it can only serve to start mapping some of the structural parameters of this new large molecule format (Fig. 3).

While all three linker lengths that were investigated are showing a very similar average paratope to paratope distance, we reasoned that the highly constrained and pre-organized Fabs observed for linker length 5 might be detrimental during formation of the encounter complex. With the linker length 15, we observed some paratope to paratope distances above 7.5 nm that can also be observed for IgG1 [48]. Therefore, we decided to produce compounds with a linker length of 10 amino acids, representing a compromise between pre-organization and rigidity on the one hand, and sufficient flexibility to allow for moderate adjustments during bivalent receptor binding on the other hand.

2.3. Contorsbodies can be produced and purified to homogeneity by standard antibody production processes

In the supernatants obtained after transient transfection, the estimated titer of the Trastuzumab Contorsbody is 28 mg/L. The size exclusion chromatography (SEC) profile indicates 80% of the expected product, about 12% of a dimeric entity (that was isolated and confirmed as a molecule containing four identical chains), and approximately 8% high molecular weight aggregates (similar to what is usually observed for standard IgGs). Total yield of purified Contorsbody after Protein A and SEC chromatography is 16.2 mg/L cell culture. Mass spectrometry confirms the product identity and purity (Fig. S1). The expected mass of 149,898.2 confirms the dimer Contorsbody, as well as two peaks corresponding to the same product with 1 or 2 C-terminal histidines missing. A third post-translational modification was found corresponding to an additional xylose on a serine residue.

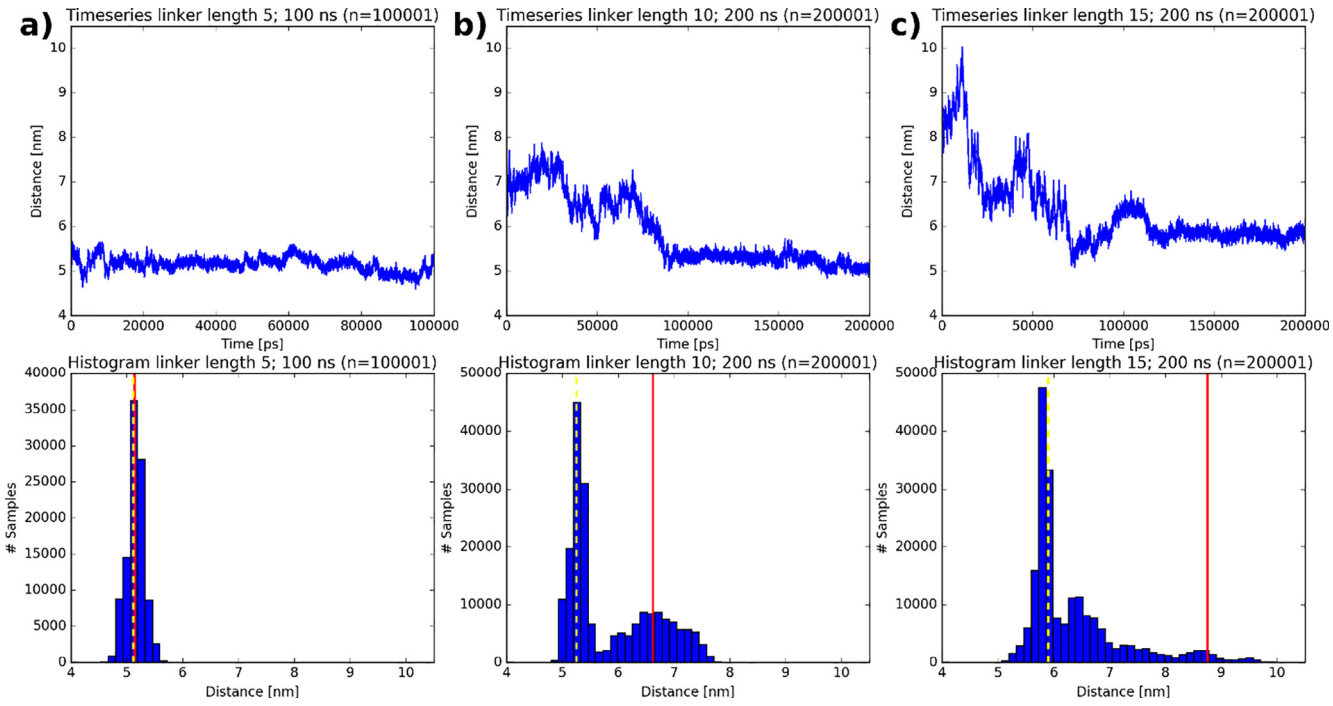

Fig. 2. Time series plots (top) and histograms (bottom) of the paratope to paratope (center of geometry) distances for Contorsbodies with a) one G4S repeat (linker length 5), b) two G4S repeats (linker length 10) and c) three G4S repeats (linker length 15). The paratope to paratope distance at simulation start is indicated with a red line. The average paratope to paratope distance over the second half of the simulation is indicated with a yellow dashed line. Given the low distance variability observed for Contorsbody with linker length 5, the simulation was suspended after 100 ns. (For interpretation of the references to colour in this figure legend, the reader is referred to the web version of this article.)

Table 1
Summary of observed paratope to paratope (center of geometery) distances for the different Contorsbody linker length variants during the MD simulation at 298 K.

	Start [nm]	Average* [nm]	Std. dev.* [nm]	Min [nm]	Max [nm]
Linker length 5	5.14	5.12	0.17	4.59	5.67
Linker length 10	6.62	5.26	0.14	4.84	7.88
Linker length 15	8.75	5.90	0.21	5.07	10.05

* Values calculated for second half of simulation.

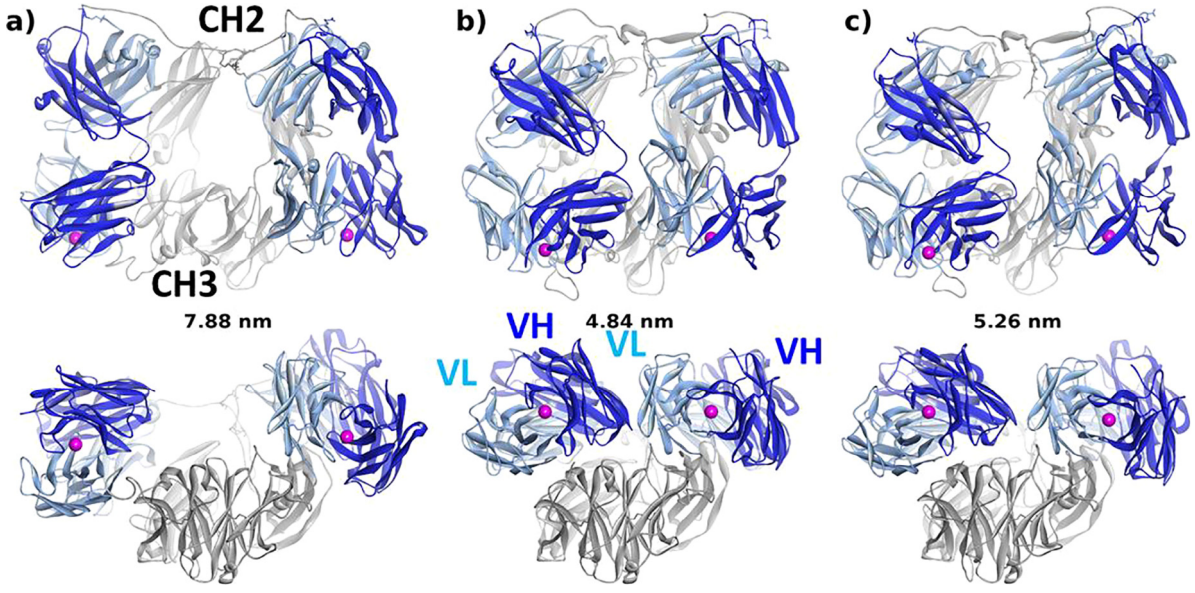

Fig. 3. Exemplary molecular states extracted from the MD simulation of the Contorsbody with linker length 10 shown in front view (top row) and bottom-up view (bottom row) representing the a) maximal, b) minimal and c) average paratope to paratope distances. Paratope centers of geometry are indicated as purple spheres. The measured distances are indicated as green dashed lines. (For interpretation of the references to colour in this figure legend, the reader is referred to the web version of this article.)

Similar observations were made for the second Contorsbody expressed (analog 2, see Table S1) with a titer of 60 mg/L compared to regular IgGs that range from 10 to 120 mg/L. A main peak of 81% was isolated by preparative SEC resulting in 33 mg of pure material from one liter cell culture.

2.4. Contorsbodies are stable entities that retain the antigen binding properties of the parent IgGs

Regular IgGs exhibit different physical properties that relate to protein folding, self-association potential, or susceptibility to temperature [17,21,43]. Changing the format might have modified those physical properties. Contorsbodies are composed of antibody-derived domains that are re-arranged via flexible linkers to assemble in a compact yet rather unusual manner. It is known that some linker-containing antibody formats (e.g. scFvs) display stability issues including increased propensity to disassemble or to form daisy-chain aggregates when compared to parental antibodies [9]. Such issues manifest themselves already early in the process with increased aggregation tendencies of desired products, or as storage/freeze–thaw incompatibilities, or in reduced thermal stability (melting temperature) of new entities compared to parent antibodies.

Purification processes did not reveal any clear tendency towards Contorsbody aggregation beyond that expected for regular IgGs (see previous section). The Fab fragment is notoriously more stable compared to the Fv portion of an antibody and contains a disulfide bridge that fixes the C-terminal ends between the CH1 and Ck domains, avoiding dissociation of the Fab for scrambling. Additionally, the Contorsbodies use relatively short linkers of 10 amino acids limiting the degree of freedom of the whole assembly. We further analyzed the thermal stability of our prototype Contorsbody using tryptophan autofluorescence. The first thermal denaturation (Tm1) is measured at 65 °C and 63 °C, for Trastuzumab and the Trastuzumab Contorsbody, respectively (Fig. S2). Assuming a high Tm of the Fc domain of about 80 °C [2], the Tm1 values observed can be attributed to the Fab domains. Thus, the Fabs linked into the Contorsbody format remain stable.

As the properties for Contorsbodies are very similar compared to regular IgGs (low aggregation tendency, no unusual storage/freeze–thaw issues observed, Tm above 60 °C), we conclude that the conversion from IgG to Contorsbody does not inflict molecular instability.

Another parameter of high importance upon converting binding entities from IgG to other formats is that their ability to bind is not compromised. Since the Trastuzumab Contorsbody molecule utilizes unmodified Fab sequences, identical CDRs (Complementary Determining Regions) are supposed to bind the receptor the same way as Trastuzumab unless a steric hindrance or a conformational modification comes into play.

Trastuzumab is an antagonist by keeping apart two Her2 extracellular domains (ECD) of the receptor; it is crucial that the new molecule is binding in a bivalent manner as we designed the Trastuzumab Contorsbody to bring two receptors together. We therefore measured the binding, i.e. the avidity, of the molecules to the Her2 ECDs via Surface Plasmon Resonance (SPR). Table 2 summarizes the avidity measurements for the two variant molecules containing the Trastuzumab binding motif. The apparent K_D value is unchanged between Trastuzumab IgG1 and Trastuzumab Contorsbody. The other apparent kinetic parameters, K_a, K_d, and $T_{1/2}$, as well as the occupation ratio, R_{max}, are also very similar for the two molecules, indicating that both molecules are binding bivalently two monomeric Her2 ECD. Sensograms are available in the supplemental material (Fig. S3). The transformation of Trastuzumab IgG1 into the Trastuzumab Contorsbody does not influence the binding capability of the new molecule.

2.5. Compact Contorsbodies have their antigen-binding regions tethered in close proximity to each other

Antibody-like molecules have natural, but flexible, linkers, e.g. around the hinge region, or even contain glycine-rich linkers used to fuse additional domains. Consequently, full IgG-based entities are difficult to crystallize; only four IgGs structures have been solved by x-ray crystallography up to now [44]. However, IgGs intrinsic flexibility can be visualized by relatively simple methods like negative staining transmission electron microscopy (NS-TEM) [48]. In addition to NS-TEM, cryo-TEM microscopy followed by 3D single particle reconstruction can help to reveal the overall architecture of the Contorsbodies. The EM studies were performed on the analog 2 Contorsbody molecule.

The Contorsbody is spatially compact compared to a regular IgG, but the introduced linkers might still account for flexibility. We first investigated the Contorsbody with and without an anti-Fc Fab to help identifying the different moieties of the molecule by NS-TEM (Fig. 4). At such relatively low resolution, the Fc region is difficult to identify with certainty. Therefore, we labelled the Fc region to enable its clear discrimination from the Fabs. The anti-Fc Fab class averages determined from micrographs recorded with NS-TEM reveal the morphology of the Contorsbody. Due to preferential binding of the molecule to the carbon film, top views were predominantly observed in raw micrographs in both experiments (Fig. 4). Three central moieties, two Fabs and one Fc, are bundled as tri-spot Contorsbody assemblies in all classes. The anti-Fc Fab is labeling the Fc Contorsbody in a 1:1 stoechiometry; The Fc part looks like a more diffuse spot, while the Contorsbody Fabs are generally more brighten than the Fc. The distance between all three moieties is overall constrained but not entirely constant. The distance between the two Fabs can be estimated to be 6–8 nm; those values are in agreement with our MD study.

The Contorsbody compactness is confirmed by NS-TEM as a "three cylinders" orientation. In addition, Cryo-EM was applied on the analog 2 Contorsbody to reconstruct the overall conformational architecture of the Contorsbody in real space (Fig. 5 and Table S2). 2721 micrographs were recorded and 214,494 extracted particles are clustered in 2D classes and further processed from an initial spherical model to reconstruct ten particle density maps (3D cryo-EM maps). All classes confirmed the compact structure already indicated with NS-TEM, but reveal several 3D conformations under cryogenic-preserved conditions, i.e the tri-spots assemblies shown at the bottom of Fig. 5.

Due to the observed flexibility, it is not possible to exclude that the Contorsbody populates a continuous conformational landscape, where moieties can swing between most closed and opened but overall constrained conformations modes. We isolate those two conformations with their envelopes at a 10 Å resolution

Table 2
Apparent Kinetic interaction parameters for the Trastuzumab Contorsbody binding Her2 vs. Trastuzumab IgG.

In solution	k_a (M^{-1} s^{-1})	k_d (s^{-1})	$t_{1/2\ diss}$ (min)	K_D (M)	R_{max} ratio (%)
Trastuzumab IgG1	1.1E + 06 ± 0.3%	<1.0E−04 ± 3.3%	>115.5	<9.1 E−11	96.1
Trastuzumab Contorsbody	1.0E + 06 ± 0.3%	<1.0 E−04 ± 0.6%	>115.5	<9.6 E−11	98.5

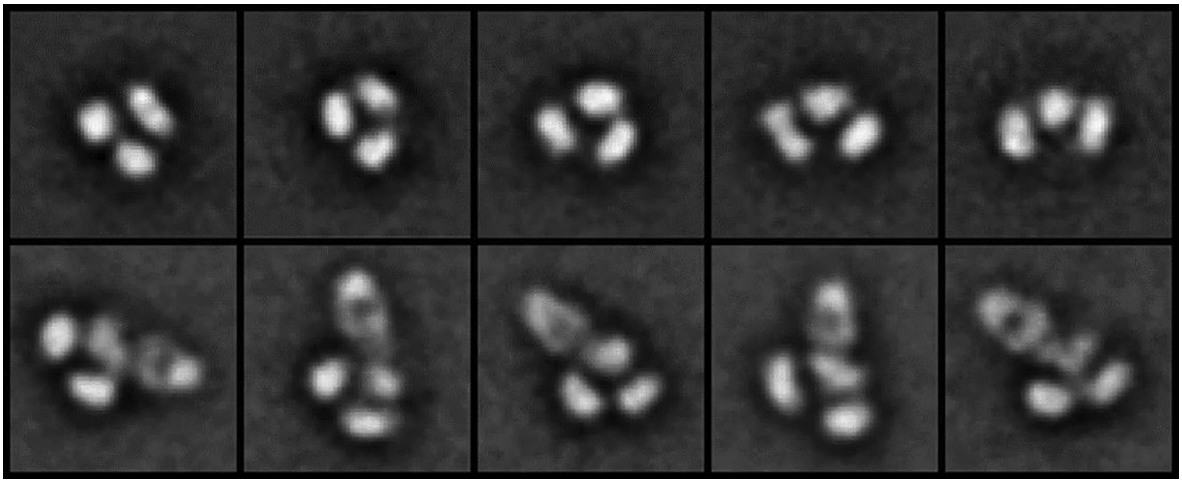

Fig. 4. NS-TEM representative 2D classes (23.6 × 23.6 nm) of the analog 2 Contorsbody. Top row: representative 2D pictures of the Contorsbody molecule alone. Bottom row: representative 2D pictures of the Contorsbody molecule in complex with an anti-Fc Fab showing that the Fc part of the Contorsbody is recognized by one anti-Fc Fab. In both rows, the Fc moiety is often assignable as the most blurry part of the assembly.

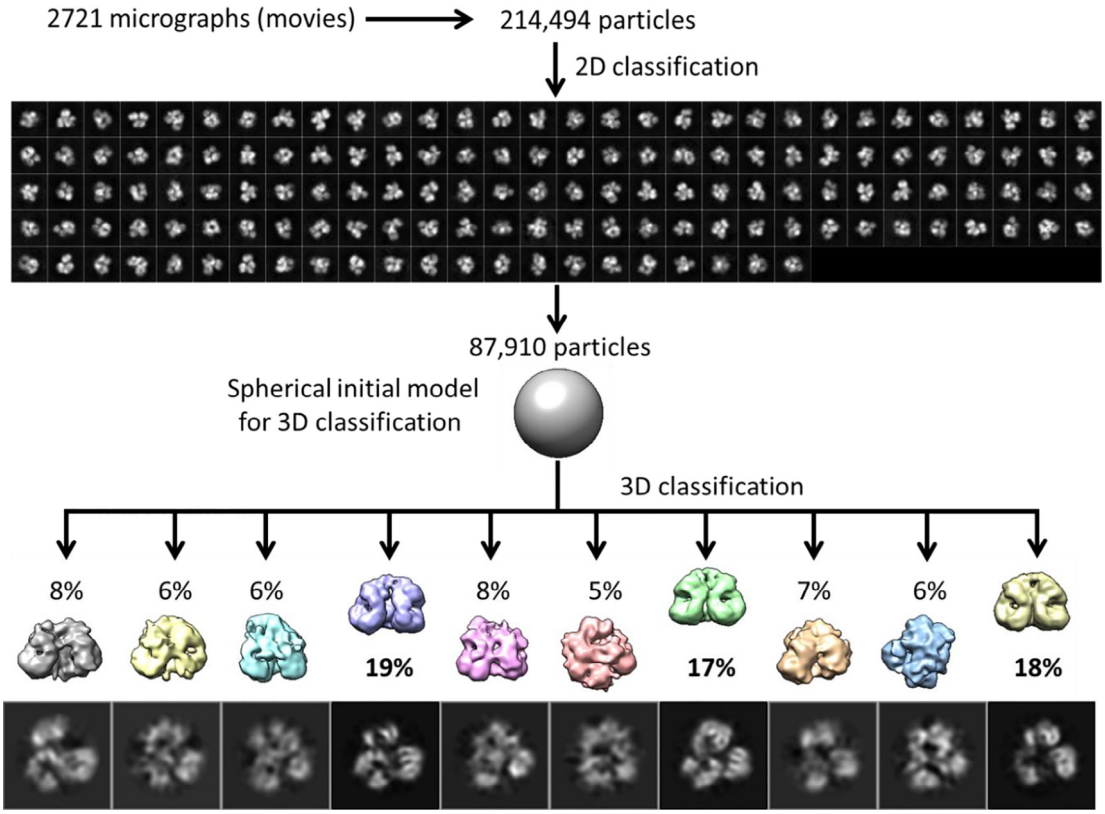

Fig. 5. Cryo-EM procedure to obtain cryo-EM maps of Contorsbody analog 2, i.e. a 2D classification of all the selected particles followed by a 3D classification into 10 classes. Three prominent 3D classes are containing 17, 18, and 19% of the particles.

(Fig. 6A). This resolution is obviously not sufficient to be able to assign each and every loops at the atomic level but the observed densities are assignable to structural domains and even some linking moieties.

Notably, the location of the hinge region with the disulfide bridges is now recognizable. The envelopes on the top views (Fig. 6D) of the open and closed conformations form a three-pointed star that makes the connection between the two narrow endings (C-termini of the Fabs) and the hinge center (see also the video in Supplementary Material). From the hinge center, two tiny linkers are forming the link to the two CH2 domains of the Fc moiety. The latter is also clearly assignable as it forms a slightly more open and diffuse doughnut-like envelope (Fig. 6C) compared to the Fabs envelopes (Fig. 6A) that seems to be more compact and less flexible. While a Fab, and especially the Fv portion of it, has to be quite rigid to ensure effective and selective antigen recognition, the Fc portion has a biologically relevant conformational plasticity [31,45]. The Fc moiety interacts with several Fc-γ receptors through the hinge and the sugar structure built on the asparagine 297 of the CH2 domain. The

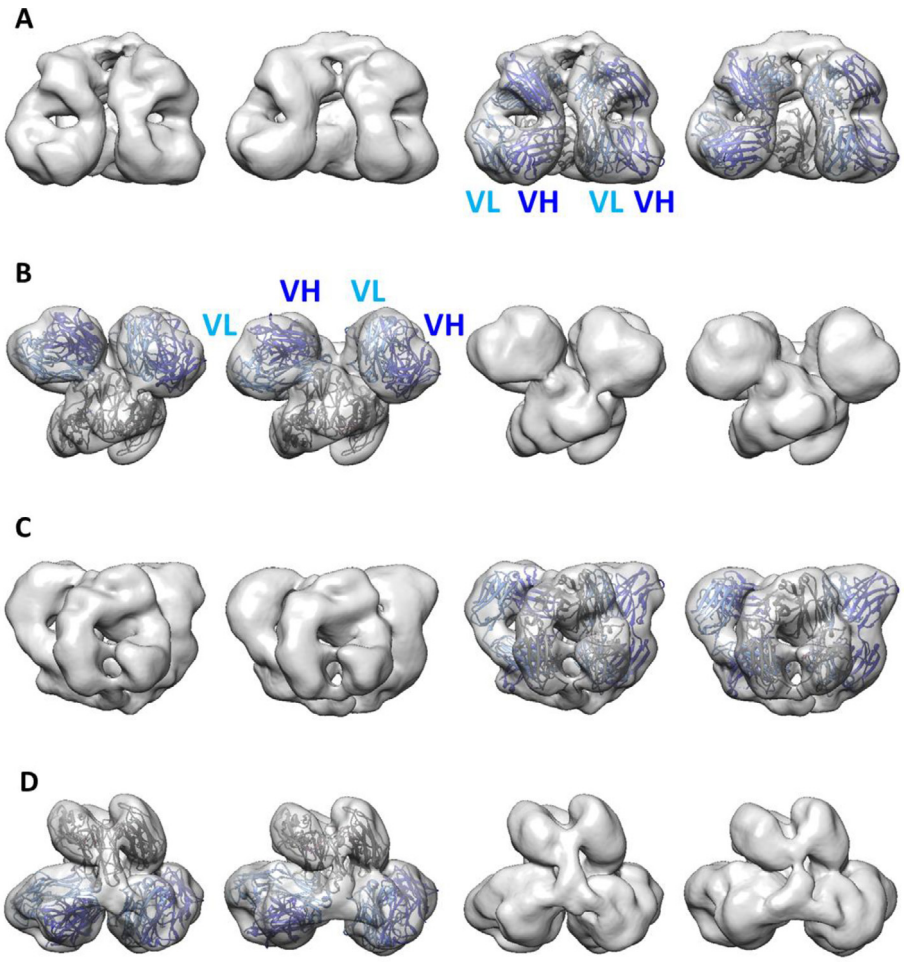

Fig. 6. Cryo-EM reconstitution of the Contorsbody 3D envelopes at 10 Å. The grey envelopes depict an open and a closed conformation in each row. In each row, a second representation shows the VH-CH1 ribbon Fab half, colored in dark blue, and the partner VL-Ck ribbon Fab half, colored in light blue. Grey ribbons of the Fc portion complete the overall architecture. A: Front view showing the two Fabs, B: Bottom view showing the Fab CDRs and the dimeric CH3 domains. C: Back view with the Fc moiety in front. D: Top views with the hinge region in front. (For interpretation of the references to colour in this figure legend, the reader is referred to the web version of this article.)

glyco-structure is heterogeneous and the type of sugar tree influences the interaction with partners [34].

While the Fc moiety envelope is distinguishable from a Fab envelope, the hinge region and the sugar moieties are not well resolved. Consequently, it is difficult to predict an interaction with the Fc-γ receptors. In contrast, the interaction with the neonatal Fc receptor (FcRn) is predictable from the EM models. The FcRn is binding the Fc elbow region between CH2 and CH3. The superimposition of the closed Contorsbody format model on the complex structure FcRn-Fc (PDB ID 4N0U [28] reveals that at least one Fc elbow region of the Contorsbody is exposed and can accommodate for FcRn binding (Fig. S5).

With a resolution of 10 Å, it is feasible to dock the Fab 3D structures of the parental antibody Fab fragment (PDB ID 4LIQ) into the two envelopes of the Fab fragments. We assume that the produced analog 2 has structurally similar Fabs compared to the parental Fab structure as the two Fv regions are two different humanized variants of the same parental antibody. The CH1-Ck packing is different from the one of VH-VL so that an unambiguous assignment of the Fab orientation is possible. However, assigning the linkage of the Fab to the hinge unambiguously at the amino acid level as well as the exact nature of the loops that form the antibody paratope recognizing specifically the antigen is extremely difficult at this resolution. Thus, the quality of the fit between Fab structure and envelope is calculated for both orientations of the VH-CH1 and VL-Ck of each Fab (Fig. S4). For both Fabs, the best correspondence was chosen as the final conformation for the analog 2 Contorsbody as depicted by the ribbons in Fig. 6.

2.6. Investigating Fab orientation in the Contorsbody

Analyzing the relative orientation of the Fabs to each other, one realizes that they are positioned more or less side by side. Taking the variable domains in Fig. 6A from the left to the right side, the VL1-VH1 pair is followed by the VL2-VH2 pair; the two Fabs show then a similar adjacent orientation. In the "Lego" structure (Fig. 1A), they are simply mirrored in a symmetrical way. In our original model, they were already positioned intuitively in an adjacent manner (Fig. 1D). To confirm this observation, we revisited the linkers and their anchoring points on the three structurally well-defined moieties, i.e. the two Fabs and the Fc part (Fig. 7).

On the top of the Fc part (Fig. 7B), the presence of the disulfide bridge between the two cysteines at the C-termini of the CH1 and the Ck domains defines precisely the anchoring points at the end of the Fab as structurally centered. The hinge is depicted with its double disulfide bridge of the human IgG1 isotype. The linkers connecting the hinge residues can then be viewed as pleated on the three cylinders as suggested by the cryo-EM envelopes (Fig. 6D).

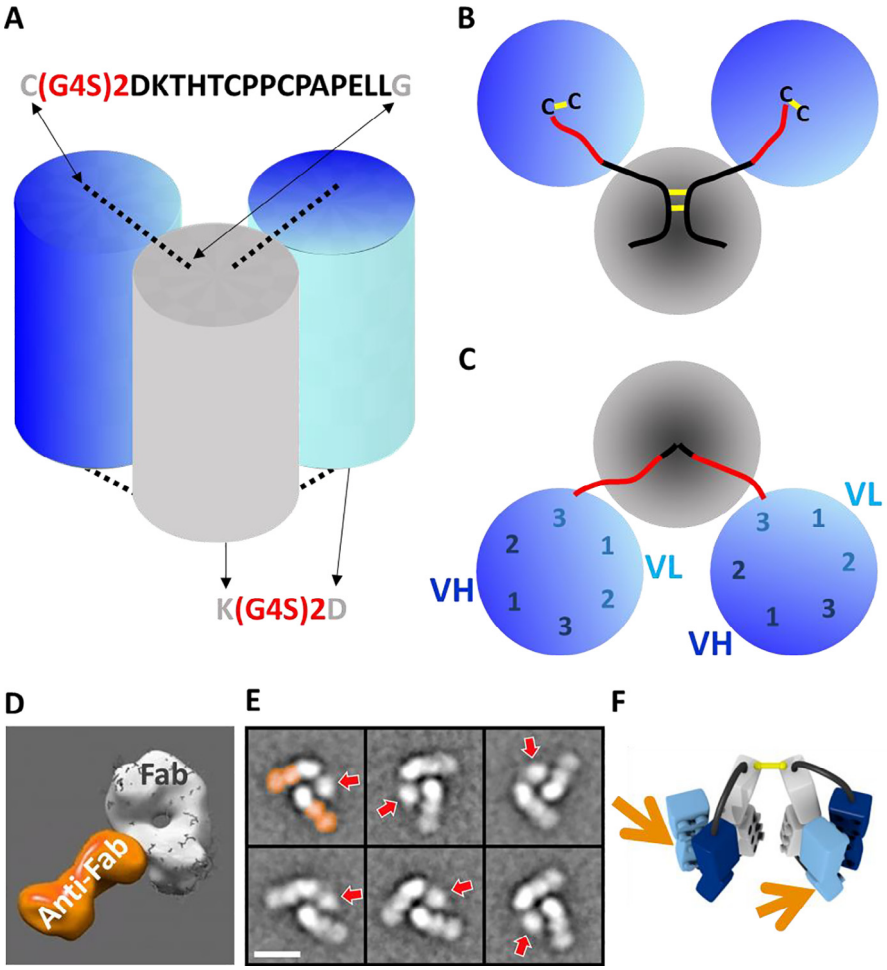

Fig. 7. A: a schematic representation of the Contorsbody architecture with written sequences corresponding to linkers (red) and less structured regions of the Contorsbody (bold). B: top view depicting the flexible linkers (red for (G4S)2 and black for regular sequence as indicated in A). Disulfide bridges are indicated in yellow. C: bottom view depicting the CDRs and their assembly to form a paratope. The red (G4S)2 is the only flexible part that connects the C-terminus of the Fc with the N-terminus of the VL, located in the back to CDRL3. D: Model structure of the anti-Fab Fab recognizing the constant part of a Fab. E: Negative staining TEM representative 2D classes of the complex between the anti-Fab Fab and the analog 2 Contorsbody showing only a type of helical arrangement of two anti-Fab (orange) with one Contorsbody (red arrows point to the Fc moiety, scale bar represents 10 nm). F: Lego translation of the previous observation with the orange arrows symbolizing the anti-Fab Fab moiety in complex with the Contorsbody. (For interpretation of the references to colour in this figure legend, the reader is referred to the web version of this article.)

From the hinge side, top of the Contorsbody architecture, the two Fab cylinders appear to freely rotate on their main axis without any preference for a specific Fab orientation.

On the opposite side (Fig. 7C), the linkers connect the C-termini of the Fc to the N-termini of the VL-Ck moieties of the Fabs. In a regular Fab or Fv structure, the N-terminal segment is located on the outer part of the binding site composed by the six CDRs, three from each of the two variable domains. More precisely, the N-terminus of a variable region is located behind the CDR3, i.e. the CDRL3 in our Contorsbody format. Thus, a free rotation of the Fab cylinders is no more expected because the anchoring point is not centered on the structured VH-VL assembly. An antibody paratope is made of 6 CDRs anchored clock wisely on two variable frameworks [9]: H1-H2-L3-L1-L2-H3 (Fig. 7C). As the chosen linkers are relatively short, i.e. 10 amino acids of (G4S)2, the constrained Fab orientation relative to the Fc leads to a side by side or adjacent Fabs. This orientation is confirmed by NS-TEM experiments using an anti-Fab Fab moiety directed to the light chain (Fig. 7D); the complex with the analog 2 Contorsbody reveals that the anti-Fab Fab is binding both Contorsbody Fabs from the left or the right side depending on the orientation of the complex on the grid (Fig. 7E). Thus, the adjacent orientation of the two Contorsbody Fabs as schematically depicted in Fig. 7F, is confirmed. The last representation differs from the lego description in Fig. 1A where the Fabs are mirrored on each side of the Fc but is in agreement with our first Contorsbody model (Fig. 1D).

2.7. Format defines function: Switching Trastuzumab from IgG to Contorsbody converts its functionality from antagonism to agonism

Receptor tyrosine-protein kinase Her2 (Human epidermal growth factor receptor 2) over-expression has been shown to play an important role in the development and progression of breast cancer [22]. The natural trigger of Her receptor signaling is ligand binding mediated dimerization [29]. Trastuzumab is a bivalent IgG with two Fab arms that bind Her2 and blocks the Her2 signaling pathway [40], leading to cell death in Her2-expressing tumor. Possible modes of action of Trastuzumab include inhibition of Her2 ECD shedding, activation of antibody-dependent cellular cytotoxicity (ADCC), and receptor down modulation [39]. However, the anti-proliferative antagonistic functionality is mainly attributed to an antibody-mediated interference with Her2 signaling. Trastuzumab is neither a ligand blocker (domain one and three) nor a binder of the dimerization interface (domain two); it binds to the fourth domain, the membrane proximal domain (Fig. S6).

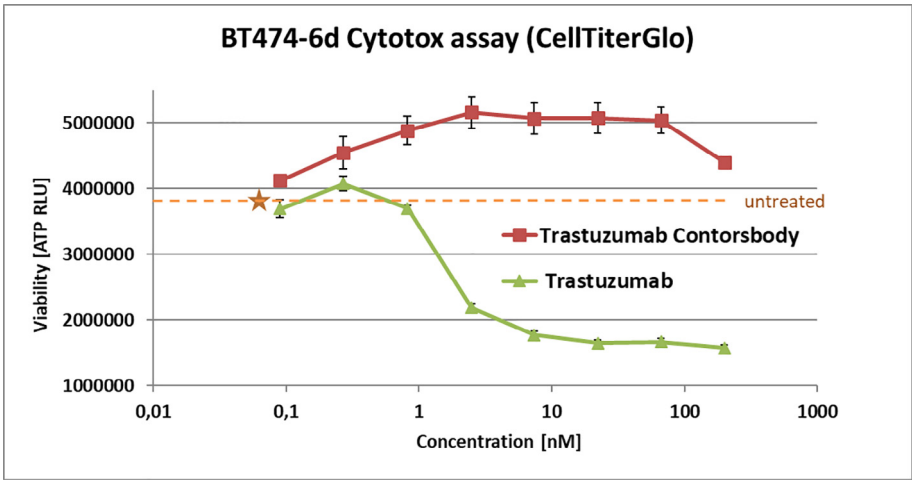

Fig. 8. BT474 cell proliferation upon treatment with Trastuzumab IgG (green curve) and Trastuzumab Contorsbody (red curve). (For interpretation of the references to colour in this figure legend, the reader is referred to the web version of this article.)

At the molecular level, we are then speculating that Trastuzumab is keeping the Her2 receptors apart.

The Trastuzumab Contorsbody is composed of the same binding and Fc modules as an IgG, yet with Fab arms constrained and tethered adjacent to each other in a tight format. This change (in format only) inverts the antagonistic functionality of Trastuzumab to deliver agonistic functionality, i.e. a pro-proliferative effect (Fig. 8). Agonistic functionality due to format change can be explained by Contorsbody mediated crosslinking of two Her2 receptors, resulting in subsequent dimerization-induced signaling.

The antibody-mediated dimerization by Her2 binding is likely similar to the one previously observed by Scheer et al. with the bis-Fabs [36]. A structural model assembly of a Her2 receptor dimer upon binding of a bis-Fab (Fig. 9) shows how a 15 Å chemical linker between two Trastuzumab Fabs can promote receptor intracellular domain dimerization.

The various bis-Fabs in the study of Scheer et al. provided a complete spectrum of functionality ranging from the F(ab)2 antagonism (similar to the IgG Trastuzumab effect) to the most agonistic bis-Fab. The functionality was dependent on the position of the cysteine introduced in the Fabs; the free cysteines are used to chemically link two Fabs. As seen in Fig. 1A, the bis-Fab molecule is still a flexible molecule. The agonistic bis-Fabs had a linker anchored closer to the paratope, i.e. in the variable region, so that the Fabs were close enough to each other in order to bring two receptors together and promote intra-cellular signaling. In contrast, the Contorsbody format provides constrained parallel Fabs along the Fc moiety and, in addition, the adjacent orientation of the variable regions, VH-VL-VH-VL or VL-VH-VL-VH, enables a cis interaction with two receptors on the same cell surface. Reverting one of the VH-VL towards a more mirrored arrangement of the Fabs would revert one of the blue-red arrow pointing to the cell surface side of one receptor, thus reducing potentially the ability of the Contorsbody to act in cis, or even favoring a bridging of two cells wearing the Her2 receptor (Fig. 9D).

3. Conclusions

In this article, we describe the design, generation and characterization of a novel antibody format. As we aimed to engineer a constrained format, the nature of the linkers used have been analyzed first by theoretical methods; one linker length of ten amino acids has then been adopted for producing the real molecules. The expression and purification of Contorsbodies are performed with the same protocol and methods that are used for regular IgGs. Titers, yields, and biophysical properties of the Contorsbodies are comparable to their parent IgGs. Furthermore, we demonstrate that the transformation of Trastuzumab into Contorsbody Trastuzumab does not affect its binding capability. In a proliferation assay, however, the functional effect of the Trastuzumab Contorsbody is drastically different. While Trastuzumab triggers significant apoptosis in the population, the Contorsbody enhances cellular proliferation.

By combining different techniques, the overall architecture of the Contorsbody has been revealed showing features like compactness, constraints to bring two Fabs together, but also a remaining flexibility with two main conformations. As the Fabs are adjacent in this architecture, they are well suited to dimerize receptors on a single cell surface.

The Contorsbody is a compact format with novel properties. i.e. agonism. It is also amenable to the generation of bispecifics through the use of the KiH technology [2], allowing to heterodimerize receptors. Other applications are conceivable to achieve targeting and recruiting of receptors using a bispecific entity or to initiate networking of a receptor using a bi-paratopic Contorsbody.

4. Materials and methods

4.1. Structural modeling and molecular dynamics

Models of the Contorsbody with different linker lengths were generated with BIOVIA Discovery Studio 17R2 [6] based on the X-ray crystal structures of a full length IgG1 (PDB ID 1HZH) [35] and Trastuzumab Fab (PDB ID 1N8Z) [10]. The models were parameterized for the AMBER99SB-ILDN forcefield [19] with residue protonation states assigned as expected normal for pH 7. All simulations were performed using the GROMACS 2019.3 software [1]. The models were solvated with explicitly modeled water (TIP3P water16 model [14]) in rhombic dodecahedron boxes with a minimum solute to box distance of 0.9 nm. To neutralize the total charge of the systems, an adequate amount of neutralizing ions was added to the simulation boxes. The energy of the systems was minimized with the steepest descent algorithm, and 100 ps position restrained MD simulations were performed to settle the solvent molecules before the unrestrained 100 or 200 ns simulations were started. To maintain a constant temperature of 298 K and a pressure of 1 bar, Nose-Hoover temperature coupling [12]

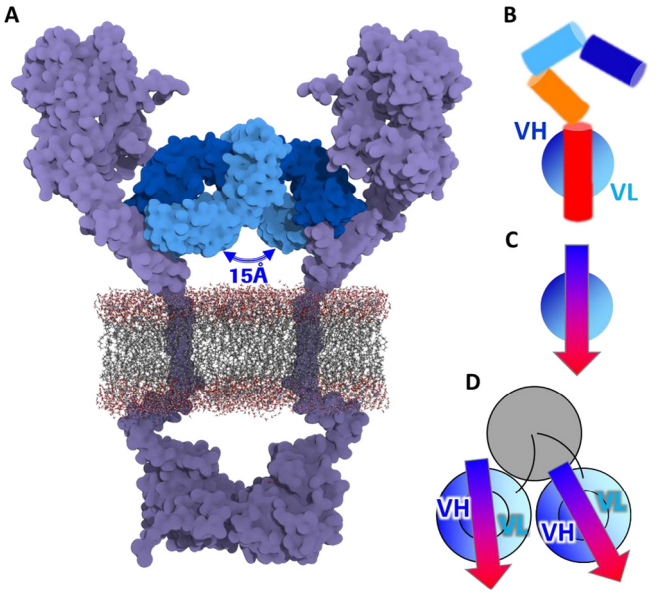

Fig. 9. A. One possible conformation of a bis-Fab of Trastuzumab [36] (heavy chain in dark blue and light chain in cyan) on two Her2 receptors (in violet) showing an on scale representation of 2 intra-cellular domains coming in contact to promote a signal transduction for growth. B: schematic representation showing the top of the Fab, i.e. the paratope, binding to the Her2 receptor. C: same view with an arrow colored by N- to C-terminus (blue to red) representing the Her2 ECD. D: the Contorsbody architecture brings two adjacent Fabs and, consequently, fixes two receptors side-by-side. (For interpretation of the references to colour in this figure legend, the reader is referred to the web version of this article.)

and Parinello-Rahman pressure coupling [25] were applied. The Smooth Particle-Mesh Ewald algorithm [11] was used for Coulomb interactions. Bond lengths involving hydrogen atoms were constrained using the LINCS algorithm [13] allowing for an integration step of 2 fs. For paratope to paratope distance calculation, the paratope position was defined as the center of geometry of all amino acid residues that were assigned to the antibody CDRs as defined by the WolfGuy [3] antibody numbering scheme.

4.2. Expression, purification, and analytics of Contorsbodies

To generate Contorsbodies, appropriate coding sequences were generated using an in-house back-translation algorithm to obtain a nucleic acids distribution leading to optimized protein expression yields (Klostermannn, Kopetzki, Schwarz. Patent application No US2015246961A1. These were generated by gene syntheses (Geneart, Regensburg, Germany), and cloned into an expression vector suitable for expression in human embryonic kidney (HEK) cells growing in suspension. The Contorsbody gene was synthesized with a 5′-end DNA sequence coding for a leader peptide, which targets proteins for secretion in eukaryotic cells, and 5′-NcoI and 3′-NheI restriction sites. Maxiprep (Qiagen) DNA preparations were used to transfect human embryonic kidney FreeStyle™ 293-F cells (Invitrogen) growing in in F17 expression medium (Gibco) at 37 °C/8% CO_2, using cells that were seeded in fresh medium at a density of 1-2×106 viable cells/ml on the day of transfection. DNA-293free™ complexes were prepared in Opti-MEM™ I medium (Gibco) using 666 μl of 293free™ (Merck) and a total of 500 μg plasmid DNA for 500 ml final transfection volume. Contorsbodies were secreted into cell culture supernatants which were harvested 7 days after transfection.

Contorsbodies were purified by capture from the supernatant via the Fc part on a Protein A column equilibrated in 1×PBS, pH 7.4. After elution with 50 mM sodium acetate, pH 3.2, the pH of the eluate was adjusted to pH 6.4. The sample was concentrated and loaded onto a preparative size exclusion chromatography column (Superdex®200 Prep Grade (GE Healthcare) equilibrated in 20 mM histidine/140 mM NaCl, pH 6.0 as polishing step.

For protein analysis by mass spectrometry, protein aliquots (50 μg) were deglycosylated by adding 0.5 μl N-Glycosidase F (Roche, 13.4 U/mL) and sodium phosphate buffer (0.1 M, pH 7.1) to obtain a final volume of 115 μl. The mixture was incubated at 45 °C for 2 h. Deglycosylated samples were desalted by size exclusion chromatography (Sepharose G-25, 40% acetonitrile with 2% formic acid). ESI mass spectra (+ve) were recorded on a Q-TOF instrument (maxis, Bruker) equipped with a nano ESI source (TriVersa NanoMate, Advion).

4.3. Stability and binding analyses

Thermal stability was measured via auto-fluorescence of tryptophan detected by a static light scattering using a laser at 266 nm and 473 nm. The aggregation temperature (Tagg) and the melting temperature (Tm) are the results of the experiment performed with a temperature ramp of 30 °C to 90 °C and 0.1 °C/min steps. Small glass cuvettes of 9 μl volume per samples are used and the concentration of the samples was 1 mg/mL. Samples buffer was 20 mM Histidin, 140 mM NaCl at pH6.0. The reference molecule Subcuvia was used to calibrate each run. Data processing was executed by the software UNcle (UNCHAINED LABS).

Interactions of the Trastuzumab Contorsbody interaction with Her2 ECD were characterized using SPR (Surface Plasmon Resonance). Monomeric Her2 ECD was reversibly captured on a CM5-sensor surface via amine coupled Omnitarg (Pertuzumab). Her2 binds to Omnitarg with a non-competing epitope which allows monitoring Trastuzumab Contorsbody binding kinetics with Her2. This assay set-up enables measuring the avidity vs. affinity as the multivalent binding is essential from the biological perspective.

Omnitarg was immobilized on the CM5-sensor surface with the usual EDC/NHS-amine coupling chemistry, an Omnitarg density of 800–1000 RU was reached. Her2 interactions were analyzed at a temperature of 25° using classical concentration series for Trastuzumab Contorsbody and Trastuzumab IgG as control with increasing concentrations of c = 3.7–300 nM. Regeneration was performed with 10 mM Glycine pH2.5 with 1 min contact time. All experiments were performed on a Biacore T200 instrument (GE Healthcare) in running buffer (PBS-Tween®20 0.05%). Samples were diluted in running buffer supplemented with 0.1% BSA. Data were evaluated with BIAevaluation Software 4.1 (GE) or Scrubber 2.0c. Binding signals were double referenced against blank buffer and a flow cell containing no Her2.

Apparent kinetic constants (Table 2) were calculated from fitting to a 1:1 Langmuir binding model (RI = 0) as an approximation. Listed KD values represent apparent avidity values, due to potential bivalent binding. The Ratio Rmax is defined as Rmax experimental/Rmax theoretical, where 100% theoretical response maximum is calculated based on the Her2 capture level (as the Resonance Units are directly proportional to molecular weight), with two binding sites for Trastuzumab IgG or Trastuzumab Contorsbody. Sensograms are available in the supplement (Fig. S3)

4.4. Structural analyses

All EM studies have been performed using the Contorsbody analog 2 (Table S1).

4.4.1. Negative staining transmission electron microscopy (TEM)

Antibody detection Fabs. Monovalent Fab fragments directed against human Fc part were provided by AbD Serotec with a concentration of 1.2 mg/mL. In particular, AbD23918.1 provided the best pictures as a single anti-Fc labeling of the Contorsbody.

A monoclonal antibody mouse anti human IgG, obtained from Thermo Fisher Scientific, was used to prepare isolated Fab domains using a Fab preparation kit (Pierce™, Thermo Fisher Scientific). The isolated Fab domains were concentrated using Vivaspin®500 (MWCO 10 kDa) and buffer exchanged to PBS (pH7.4) to a final concentration of 1.4 mg/mL. The resulting anti-Fab Fab is recognizing the Ck domain.

Grid preparation. Sample volumes of 4 μl at concentrations of about 5 μg/ml were adsorbed to glow discharged carbon coated 400 mesh copper TEM grids. After 20 s, liquid was blotted off with blotting paper and the surface immediately washed with five droplets of double-distilled water. Finally, the surface was negatively stained with two droplets of 2% uranyl acetate in water, excess liquid was blotted of and the grids dried in air.

TEM. Data were collected with either a Tecnai12 TEM or a CM 100 TEM (FEI Philips, Eindhoven, the Netherlands) both equipped with LaB6 filaments, operated at 120 kV or 80 kV respectively. Electron micrographs taken on Tecnai12 TEM were recorded on a 4096 by 4096-pixels charge-coupled device camera (TVIPS F416) at various nominal magnifications yielding a final pixel size between 0.25 and 0.426 nm on the specimen level. Electron micrographs taken on CM100 TEM were recorded using 2048 × 2048-pixels side-mounted TEM charge-coupled device camera (Veleta, Olympus soft imaging solutions GmbH, Münster, Germany).

Image processing. Reference-free alignment was performed on manually or automatically selected particles from recorded images using the EMAN2 image processing package [20]. The extracted particles were aligned and classified by multivariate statistical analysis yielding 2D class averages.

4.4.2. Cryo electron microscopy

Grid preparation. Cryo-EM grids were prepared using a Vitrobot Mark IV (FEI) with 100% humidity at 4 °C. Cryo conditions were optimized by exchanging the buffer of the stock protein solution to D-PBS (Gibco Life Technologies) and diluting to about 1 mg/ml. Aliquots of 2 μl diluted sample were placed on both sides on glow-discharged lacey C only 400 mesh TEM grid. After blotting with Whatman paper for 3 s, grids were plunge frozen in liquid ethane cooled by liquid nitrogen.

Data acquisition. Micrographs were acquired on a Titan Krios (ThermoFisher Scientific) transmission electron microscope, operated at 300 kV and equipped with a Gatan Quantum-LS imaging energy filter (GIF, 20 eV zero loss energy window; Gatan Inc). Images were recorded on a K2 Summit electron counting direct detection camera (Gatan Inc) in dose fractionation mode (40 frames over 16 s) using the Serial EM software [23] at pixel sizes 0.1058 nm ending up in a total dose of ~80 electrons per square Angstrom (e−/Å2) for each micrograph. Micrographs were processed and analyzed during data collection with FOCUS [5], applying drift-correction and dose-weighting using MotionCor2 (Zheng et al., 2017).

Image processing. The drift-corrected, dose-weighted micrographs were imported from Focus into RELION-2.1-beta-1 [37], using sciCORE, the scientific computing core facility at University of Basel. Contrast transfer function (CTF) parameters were estimated with GCTF [47]. Particles were picked using Gautomatch (Urnavicius 2015) and a template prepared with a negative stain 3D model low pass filtered to 40 Å and projected in evenly spaced (15°) directions. A total of 214,494 particles were then picked from 2721 electron micrographs. After several rounds of 2D classification, 3D classification and selection of particles, the data set was reduced to 22,736 particles. These particles were used to perform a final 3D classification, yielding to two maps (open and closed) with resolutions of around 10 Å by FSC using the 0.143 Å cut-off criterion [8,33,37]. Alternatively, 87,910 particles similarly also selected from 2D classification rounds, were submitted to 3D classification in 10 classes using a sphrere as a starting model. This allowed to estimate the relative distribution of the conformations.

Modeling. Two Fabs structures (PDB ID 4LIQ [32]) and one Fc (PDB ID 1HZH [35]) were successively placed into the cryo-EM maps and fitted using the UCSF Chimera software package. The final partial models missing the linker parts (G4S)2 of open and closed conformations were produced.

4.5. Cellular proliferation assay

Pre-cultured human BT474 cells (Her2 + breast cancer cell line, ATCC, HTB-20) were seeded at 1×10^4 cells/well (96-well flat bottom plate), cultured overnight in standard medium (RPMI/10% FCS), before adding Trastuzumab and Trastuzumab Contorsbody at different concentrations for subsequent incubation during six days and determination of Cell viability/proliferation (CellTiter-Glo® Luminescent, Promega, Walldorf, Germany). Briefly, 100 μl growth medium was removed and 100 μl CellTiterglo Reaction Mix was added to the cells and incubated for 2 min on an orbital shaker. After thorough homogenization, 100 μl cell lysate was transferred to a new 96-well plate (white) and mixed before luminescence measurements were performed using a TECAN reader.

Acknowledgments

GG thanks Ute Jucknischke, Diana Pippig, and Alexander Knaupp for their contribution to SPR and stability data. FP thanks Hermann Beck for providing the anti human IgG_Fc Fab fragment. The authors are grateful to Jack Bates for his contribution as native speaker.

Authorship contributions

GG is the originator and initiator of the Contorsbody concept. GG, SD, UB and SI-J contributed to generation & characterization of Contorsbodies, expansion of Contorsbody concepts and prepared the manuscript. AG, FH, and JAAF characterized the prototypic Contorsbodies. All others contributed to structural characterization of Contorsbodies and manuscript preparation.

Competing interests

All authors, except HS and PR, are employees of Roche. Roche has an interest in targeted therapies.

Appendix A. Supplementary data

Supplementary data to this article can be found online at https://doi.org/10.1016/j.csbj.2020.05.007.

References

[1] Abraham MJ, Murtola T, Schulz R, Páll S, Smith JC, Hess B, et al. GROMACS: High performance molecular simulations through multi-level parallelism from laptops to supercomputers. SoftwareX 2015;1:19–25. https://doi.org/10.1016/j.softx.2015.06.001.

[2] Atwell S, Ridgway JBB, Wells JA, Carter P. Stable heterodimer from remodeling the domain interface of a homodimerusing a phage display library. J Mol Biol 1997;270:26–35. https://doi.org/10.1006/jmbi.1997.1116.

[3] Bujotzek A, Dunbar J, Lipsmeier F, Schäfer W, Antes I, Deane CM, et al. Prediction of VH–VL domain orientation for antibody variable domain modeling. Proteins Struct Funct Bioinf 2015;83:681–95. https://doi.org/10.1002/prot.24756.

[4] Brinkmann U, Kontermann RE. The making of bispecific antibodies. mAbs 2017;9:182–212. https://doi.org/10.1080/19420862.2016.1268307.

[5] Biyani N. Focus: the interface between data collection and data processing in cryo-EM. J Struct Biol 2017;198:124–33. https://doi.org/10.1016/j.jsb.2017.03.007.

[6] Dassault Systèmes BIOVIA. Discovery Studio 17R2. San Diego: Dassault Systèmes; 2016.

[7] Carter P, Presta L, Gorman CM, Ridgway JBB, Henner D, Wong WLT, et al. Humanization of an anti-p185HER2 antibody for human cancer therapy. Proc Natl Acad Sci USA 1992;89:4285–9. https://doi.org/10.1073/pnas.89.10.4285.

[8] Chen S, McMullan G, Faruqi AR, Murshudov GN, Short JM, Scheres SHW, et al. High-resolution noise substitution to measure overfitting and validate resolution in 3D structure determination by single particle electron cryomicroscopy. Ultramicroscopy 2013;135:24–35. https://doi.org/10.1016/j.ultramic.2013.06.004.

[9] Chiu ML, Goulet DR, Teplyakov A, Gilliland GL. Antibody structure and function: the basis for engineering therapeutics. Antibodies 2019;8(4):55. https://doi.org/10.3390/antib8040055.

[10] Cho H, Mason K, Ramyar K, Stanley AM, Gabelli SB, Denney Jr DW, et al. Structure of the extracellular region of HER2 alone and in complex with the Herceptin Fab. Nature 2003;421:756–60. https://doi.org/10.1038/nature01392.

[11] Essmann U, Perera L, Berkowitz ML, Darden T, Lee H, Pedersen LG. A smooth particle mesh Ewald method. J Chem Phys 1995;103:8577–93. https://doi.org/10.1063/1.470117.

[12] Evans DJ, Holian BL. The nose–hoover thermostat. J Chem Phys 1985;83:4069–74. https://doi.org/10.1063/1.449071.

[13] Hess B, Bekker H, Berendsen HJ, Fraaije JG. LINCS: a linear constraint solver for molecular simulations. J Comput Chem 1997;18:1463–72. https://doi.org/10.1002/(SICI)1096-987X(199709)18:12%3C1463::AID-JCC4%3E3.0.CO;2-H.

[14] Jorgensen WL, Chandrasekhar J, Madura JD, Impey RW, Klein ML. Comparison of simple potential functions for simulating liquid water. J Chem Phys 1983;79:926–35.

[15] Kaplon H, Muralidharan M, Schneider Z, Reichert JM. Antibodies to watch in 2020. MAbs 2020;12:1703531. https://doi.org/10.1080/19420862.2019.1703531.

[16] Kaplon H, Reichert JM. Antibodies to watch in 2019. MAbs 2019;11:219–38. https://doi.org/10.1080/19420862.2018.1556465.

[17] Le Basle Y, Chennell P, Tokhadze N, Astier A, Sautou V. Physicochemical stability of monoclonal antibodies: a review. J Pharm Sci 2020;109:169–90. https://doi.org/10.1016/j.xphs.2019.08.009.

[18] Leavy O. Therapeutic antibodies: past, present and future 297 297. Nat Rev Immunol 2010;10. https://doi.org/10.1038/nri2763.

[19] Lindorff-Larsen K, Piana S, Palmo K, Maragakis P, Klepeis JL, Dror RO, et al. Improved side-chain torsion potentials for the Amber ff99SB protein force field. Proteins Struct Funct Bioinf 2010;78:1950–8. https://doi.org/10.1002/prot.22711.

[20] Ludtke SJ, Baldwin PR, Chiu W. EMAN: semiautomated software for high-resolution single-particle reconstructions. J Struct Biol 1999;128:82–97. https://doi.org/10.1006/jsbi.1999.4174.

[21] Ma H, O'Fagain C, O'Kennedy R. Unravelling enhancement of antibody fragment stability – role of format structure and cysteine modification. J Immunol Methods 2019;464:57–63. https://doi.org/10.1016/j.jim.2018.10.012.

[22] Marmor Mina D, Skaria Kochupurakkal Bose, Yarden Yosef. Signal transduction and oncogenesis by ErbB/HER receptors. Int J Radiat Oncol Biol Phys 2004;58(3):903–13. https://doi.org/10.1016/j.ijrobp.2003.06.002.

[23] Mastronarde DN. Automated electron microscope tomography using robust prediction of specimen movements. J Struct Biol 2005;152:36–51. https://doi.org/10.1016/j.jsb.2005.07.007.

[24] Mayes PA, Hance KW, Hoos A. The promise and challenges of immune agonist antibody development in cancer. Nat Rev Drug Discov 2018;17:509–27. https://doi.org/10.1038/nrd.2018.75.

[25] Melchionna S, Ciccotti G, Holian BL. Hoover NPT dynamics for systems varying in shape and size. Mol Phys 1993;78:533–44. https://doi.org/10.1080/00268979300100371.

[26] Mijares A, Lebesgue D, Wallukat G, Hoebeke J. From agonist to antagonist: Fab fragments of an agonist-like monoclonal anti-beta(2)-adrenoceptor antibody behave as antagonists. Mol Pharmacol 2000;58:373–9. https://doi.org/10.1124/mol.58.2.373.

[27] Natha R, Esteva FJ. Herceptin: mechanisms of action and resistance. Cancer Lett 2006;232:123–38. https://doi.org/10.1016/j.canlet.2005.01.041.

[28] Oganesyan V, Damschroder MM, Cook KE, Li Q, Gao C, Wu H, et al. Structural insights into neonatal fc receptor-based recycling mechanisms. J Biol Chem 2014;289:7812–24. https://doi.org/10.1074/jbc.M113.537563.

[29] Olayioye MA. Intracellular signaling pathways of ErbB2/HER-2 and family members. Breast Cancer Res 2001;3:385. https://doi.org/10.1186/bcr327.

[30] Reichert Janice M. Antibodies to watch in 2017. mAbs 2017;9(2):167–81. https://doi.org/10.1080/19420862.2016.1269580.

[31] Remesh SG, Armstrong AA, Mahan Ad, Luo J, Hammel M. Conformational plasticity of the immunoglobulin fc domain in solution. Structure 2018;26:1007–14. https://doi.org/10.1016/j.str.2018.03.017.

[32] Ries CH, Cannarile MA, Hoves S, Benz J, Wartha K, Runza V, et al. Targeting tumor-associated macrophages with anti-CSF-1R antibody reveals a strategy for cancer therapy. Cancer Cell 2014;25:46–859. https://doi.org/10.1016/j.ccr.2014.05.016.

[33] Rosenthal PB, Henderson R. Optimal determination of particle orientation, absolute hand, and contrast loss in single-particle electron cryomicroscopy. J Mol Biol 2003;333:721–45. https://doi.org/10.1016/j.jmb.2003.07.013.

[34] Sakae Y, Satoh T, Yagi H, Yanaka S, Yamaguchi T, Isoda Y, et al. Conformational effects of N-glycan core fucosylation of immunoglobulin G Fc region on its interaction with Fcγ receptor IIIa. Sci Rep 2017;7:13780. https://doi.org/10.1038/s41598-017-13845-8.

[35] Saphire OE, Parren PWHI, Pantophlet R, Zwick MB, Morris GM, Rudd PM, et al. Crystal structure of a neutralizing human IgG against HIV-1: a template for vaccine design. Science 2001;293:1155–9. https://doi.org/10.1126/science.1061692.

[36] Scheer JM, Sandoval W, Michael Elliott J, Shao L, Luis E, Lewin-Koh S-C, et al. Reorienting the fab domains of trastuzumab results in potent HER2 activators. PLoS One 2012;7:51817. https://doi.org/10.1371/journal.pone.0051817.

[37] Scheres SHW. RELION: implementation of a Bayesian approach to cryo-EM structure determination. J Struct Biol 2012;180:519–30. https://doi.org/10.1016/j.jsb.2012.09.006.

[38] Shi SY, Lu Y-W, Liu Z, Stevens J, Murawsky CM, Wilson V, et al. A biparatopic agonistic antibody that mimics fibroblast growth factor 21 ligand activity. J Biol Chem 2018;293:5909–19. https://doi.org/10.1074/jbc.RA118.001752.

[39] Sliwkowski MX, Mellman I. Antibody therapeutics in cancer. Science 2013;341:1192–8. https://doi.org/10.1126/science.1241145.

[40] Valabrega G, Montemurro F, Aglietta M. Trastuzumab: mechanism of action, resistance and future perspectives in HER2-overexpressing breast cancer. Ann Oncol 2007;18:977–84. https://doi.org/10.1093/annonc/mdl475.

[41] Vonderheide RH. CD40 agonist antibodies in cancer immunotherapy. Annu Rev Med 2020;71:1.1–1.12. https://doi.org/10.1146/annurev-med-062518-045435.

[42] Vu T, Claret FX. Trastuzumab: updated mechanisms of action and resistance in breast cancer. Front Oncol 2012;2:62. https://doi.org/10.3389/fonc.2012.00062.

[43] Wang W, Singh S, Zeng DL, King K, Nema S. Antibody structure, instability, and formulation. J Pharm Sci 2007;96:1–26. https://doi.org/10.1002/jps.20727.

[44] White Jay J, Bray B, Qi Y, Igbinigie E, Wu H, Li J, et al. IgG antibody 3D structures and dynamics. Antibodies 2018;7:18. https://doi.org/10.3390/antib7020018.

[45] Yageta S, Imamura H, Shibuya R, Honda S. CH2 domain orientation of human immunoglobulin G in solution: structural comparison of glycosylated and aglycosylated Fc regions using small-angle X-ray scattering. mAbs 2019;11:453–62. https://doi.org/10.1080/19420862.2018.1546086.

[46] Yanga Y, Yeh SH, Madireddi S, Matochko WL, Gu C, Pacheco Sanchez P, et al. Tetravalent biepitopic targeting enables intrinsic antibody agonism of tumor necrosis factor receptor superfamily members. mAbs 2019;11:996–1011. https://doi.org/10.1080/19420862.2019.1625662.

[47] Zhang K. Gctf: real-time CTF determination and correction. J Struct Biol 2016;193:1–12. https://doi.org/10.1016/j.jsb.2015.11.003.

[48] Zhang X, Zhang L, Tong H, Peng B, Rames MR, Zhang S, et al. 3D Structural fluctuation of IgG1 revealed by individual particle Electron Tomography. Sci Rep 2015;5:9803. https://doi.org/10.1038/srep09803.